

IMPACT CRATERING IN ICE- AND ICE-SILICATE TARGETS: AN EXPERIMENTAL ASSESSMENT
 by M. A. Lange and T. J. Ahrens, Seismological Laboratory, 252-21
 California Institute of Technology, Pasadena, California 91125

Introduction: The presence of cratered surfaces on the icy Jovian and Saturnian satellites (e.g., 1, 2) suggests comparisons with the extensively studied cratering records on the silicate terrestrial planets. Upon comparison of cratering records of different terranes on the Jovian and Saturnian satellites, a time scale for endogenic processes can be inferred for these objects (3, 4, 5). However, this procedure is complicated by the differences in physical properties of ice- and ice-silicate targets at very low temperatures (surface temperatures on the Galilean and Saturnian moons lie at 110 and 70 K, resp.) compared to those of silicates (e.g., mean density, thermodynamic equation of state, compressive- and tensile strength). Hence, application of known principles of impact crater formation in silicates to icy targets is limited. Laboratory cratering experiments provide a first step to overcome this complication. Experiments yield basic data to be used in scaling relationships and theoretical models of the cratering process.

We report results which (i) determine the dependence of major impact crater dimensions in icy targets as a function of impact energy and target temperature, (ii) compare crater formation in pure ice- and ice-silicate targets with that in silicate targets, (iii) determine the effects of varying silicate contents on crater dimensions for ice-silicate targets, and (iv) relate the experimental results to natural cratering events on icy planets.

Experimental Techniques: The experiments were performed on cylindrical targets (diameter = 20 cm, height = 17 - 20 cm, mass = 5 - 6 kg). Target preparation has been described in detail elsewhere (6, 7). Briefly, pure ice targets were obtained by freezing water in a brass container, ice-silicate targets are compressed homogeneous mixtures of crushed ice and silica sand (both with comparable grain size of 0.1 mm) with 35 - 40 wt.% sand and porosities (due to incomplete compression) of $\leq 10 - 15$ %. Two target temperatures of 257 and 81 K are achieved by either cooling the target in a freezer at 257 K or by use of boiling liquid nitrogen as a coolant. The targets are impacted by cylindrical LEXAN projectiles (density = 1.2 g/cm³) by use of a 20 mm propellant gun. Impact velocities vary between 0.14 and 0.5 km/s, impact (projectile) energies between 8×10^8 and 10^{10} ergs.

Results: The morphologies and shapes of the resulting impact craters reflect the fact that they are mainly formed by spallation of target fragments along radial fractures centered at the impact point. Intersection of radial with concentric fractures lead to the breaking of larger fragments and results in mean sizes of ejected particles generally not exceeding 1 cm. Fracture patterns in cross sections of impacted target blocks resemble those found in rock targets (e.g., 8). Fracture densities in both pure ice- and ice silicate targets at 81 K are significantly higher than in the 257 K targets. This indicates a less effective pressure attenuation in the cold targets.

Our data (Fig. 1) demonstrate that a decrease in temperature as well as the addition of silicates to pure ice leads to decreasing crater diameters for a given impact. The temperature effect is more pronounced in ice-silicates as compared to pure ice targets and leads to crater diameters in ice-silicates approaching those found in basalt as given by (9). Crater depth to diameter ratios of our targets are similar to those in basaltic rocks. Decreasing temperatures and the addition of silicates leads to decreasing crater volumes as compared to craters in pure ice (Fig. 2). Crater volumes in icy targets are up to 10^2 times as large as those in rocky targets. Crater diameters D and silicate content f_s in our experiments are related by: $D(\text{cm}) = 11.4 - 0.14 f_s$. Silicate grains in an ice matrix effectively lead to higher tensile- and compressive strength, which results in decreasing crater diameters with increasing sand content. This is in good agreement with quasi-static strength measurements by (10).

Discussion and Conclusion: The dimensionless analysis of experimental cratering data (11, 12) provides a powerful tool in defining limits for the applicability of our results. The data for our four target types define separate relations for π_1 versus π_2 (Fig. 3). Values for the peak compressive strength Y for ice and ice-silicates (37 wt.%) at 257 K as given by (10) (28 and 42 MPa, resp.) yield a relation between π_1 and π_2 : $\pi_1 \pi_2^{1.1} = 0.75$. This is used to infer $Y = 41$ and $Y = 180$ MPa for ice and ice-silicates at 81 K, resp. Since cratering in our experiments is dominated by the target strength, the water line (13) defines the upper limit of π_1 for extrapolation of our results (Schmidt, pers. comm.). Taking $\pi_2 = 5 \times 10^{-6}$ yields a π_1 of 4.5×10^{-3} and $\pi_2 = 1.9 \times 10^{-4}$ (Fig. 3). This is used to infer upper bounds for impact velocities U , based on the strength values Y for ice and ice-silicate targets. The values for π_2 and U now yield maximum impactor sizes, a , to be used in modeling impacts on a planet with surface gravity g . In order to obtain crater radii r , we determined π_1 versus π_2 for our 81 K targets (Fig. 4). Fig. 5 gives the maximum crater diameters which we can predict for cratering in icy targets at 81 K for a given combination of a , g , and U .

Usable impact velocities in our model are below those estimated for primary events on the Jovian and Saturnian satellites (4, 5). However, our results have implications for low-velocity and secondary cratering which is largely responsible for the evolution of a planetary regolith. We predict an accelerated regolith formation on icy planets as compared to silicate planets, based on the much higher crater volumes in icy targets. This has several implications for models of crater relaxation in an icy crust (e.g., 14) and for the geological evolution of an icy planet (3).

References: (1) Smith B. F., et al. (1979) *Science* 206, 927-950. (2) Smith B. F., et al. (1981) *Science* 212, 163-191. (3) Shoemaker E. M., et al. (1981) submitted to *The Satellites of Jupiter*, Univ. of Ariz. Press. (4) Shoemaker E. M. and Wolfe R. F. (1980) submitted to *The Satellites of Jupiter*, Univ. of Ariz. Press. (5) Shoemaker E. M. and Wolfe R. F. (1981) In *Lunar and Planetary*

Lange, M. A. and Ahrens, T. J.

Science XII Suppl. A, 1-3, Lunar and Planetary Inst., Houston. (6) Lange M. A. and Ahrens T. J. (1981) EOS 62, 318. (7) Lange M. A. and Ahrens T. J. (1981) EOS 62, 939. (8) Hörz F. (1969) Contr. Mineral. Petrol. 21, 365-377. (9) Gault D. E. (1973) The Moon 6, 32-44. (10) Goughmour R. R. and Andersland O. B. (1968) J. Soil Mech. Found. Div. ASCE 923-950. (11) Holsapple K. A. and Schmidt R. M. (1981) J. Geophys. Res., in press. (12) Schmidt R. M. (1980) Proc. Lunar Plan. Sci. Conf. 11th, 2099-2128. (13) Gault D. E. (1978) EOS 59, 1121. (14) Passey Q. R. and Shoemaker E. M. (1981) submitted to The Satellites of Jupiter, Univ. of Ariz. Press.

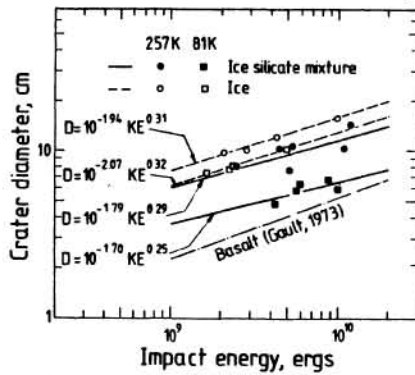


Figure 1: Crater diameters (D) versus impact energies (KE) in ice-, ice-silicate-, and basalt targets in laboratory experiments. Equations are linear regression fits to our data

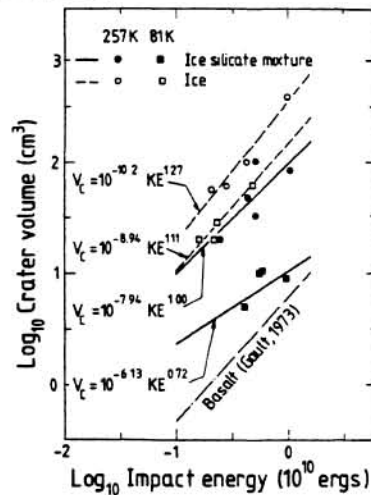


Figure 2: Crater volumes (V) versus impact energy (KE) in ice-, ice-silicate-, and basalt targets in laboratory experiments. Equations represent linear regression fits to our data

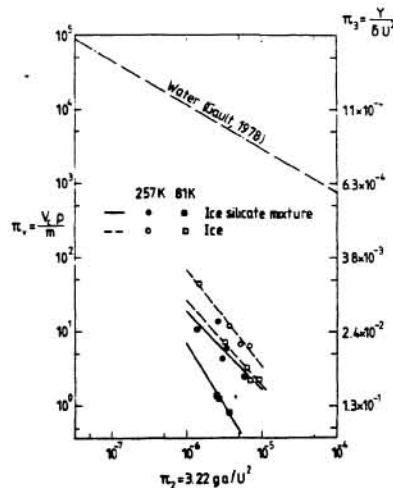


Figure 3: Cratering efficiency π for our experiments. V =crater volume; Y, ρ =target density and strength, resp.; m, a, δ =projectile mass, radius, and density, resp.; g =surface density; U =impact velocity. π_3 values based on relation between π_v and π_3 for our data (see text).

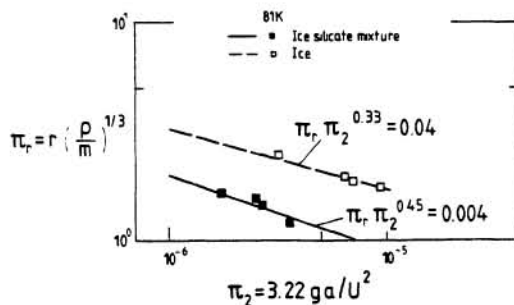


Figure 4: Scaled crater radii π_r versus π_2 for our 81K targets. r =crater radius. Equations represent linear regression fit to our data.

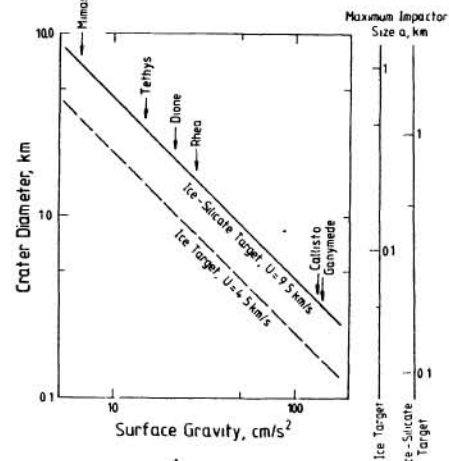


Figure 5: Predicted crater diameters, based on our results, for a given set of $g, a,$ and U . Diameter values represent maximum limits for applicability of our scaling relation given in Fig. 4. Surface gravities of Saturnian and Jovian satellites are indicated.

Acknowledgements: We would like to thank R. Schmidt for numerous helpful suggestions with regard to the dimensionless analysis of our cratering data. Technical assistance of G. Campbell is gratefully acknowledged. M. Lange is supported by a stipend of the Deutsche Forschungsgemeinschaft. This work is supported by NASA grant NGL-05-002-105.